Available online at www.sciencedirect.com

ScienceDirect

Procedia Computer Science 70 (2015) 526 – 537

Procedia Computer Science

4th International Conference on Eco-friendly Computing and Communication Systems, ICECCS 2015

Wind Speed Variation Impact on Transmission Loss Reduction in Electricity Market

Manish Kumar[a], K. S. Sandhu[b], and Ashwani Kumar[c]*

[a]*National Instituite of Technologyy, Kurukshetra, 136119, India*
[b,c]*National Instituite of Technologyy, Kurukshetra, 136119, India*

Abstract

In this paper, effect of wind speed variation on its output has been obtained and analysis has been carried out for transmission loss minimization. Mixed integer nonlinear programming (MINLP) approach has been utilized for determining optimal location and number of DFIG as distributed generators considering minimization of transmission loss. The impact of wind speed variation has also been incorporated in the optimization model for obtaining the impact of DFIG output on the transmission loss. The capability curves of DFIG have been modeled in an optimization model and impact of wind speed variation for 24 hrs has been considered to obtain the impact on DFIG output and thereby on the transmission loss. The total real and reactive power loss, optimal DG location, 24 hr optimal schedule of conventional generators and DG output has been obtained. The effect wind variation is determined on the location and output of DG. The proposed MINLP based optimization approach has been applied for IEEE 24 bus reliability test system.

Peer-review under responsibility of the Organizing Committee of ICECCS 2015

Keywords: Distributed generation, transmission loss, Mixed integer programming approach.

* Corresponding author. Tel.: +911744233389; fax: +911744238050.
E-mail address: ashwani.k.sharma@nitkkr.ac.in

Peer-review under responsibility of the Organizing Committee of ICECCS 2015
doi:10.1016/j.procs.2015.10.095

1. Introduction

In the competitive electricity markets, there has been increased interest in Distributed Generation (DG) integration. The distributed generation in the high voltage, medium voltage or at the low voltage is going to play a key role for power system operation in the near future [1]. Many authors defined DGs based on their size, location, and technologies [2-3]. The technical benefits of DG integration are well documented in [4]. The planning of the system in the presence of DGs due to the increased share will require the assessment of number and the capacity of units, best possible location in the network, and impact of DG on the system operation viz. losses, voltage profile, and stability [5]. A distributed system planning with new integrated model minimizing investment costs, operating costs and payments for compensation of losses was proposed in [6]. Many authors proposed a multi-objective optimization approaches using evolutionary algorithm for sizing and siting of distributed generation in distribution systems has been presented in [7-11]. Many authors proposed DG integration in a pool based system competitive, social welfare maximization and multi-objective optimization for DG allocation in [12-14]. Minimizing energy losses and optimal allocation of DGs for smart renewable energy sources was proposed in [15]. Authors presented distributed generation planning considering uncertainties [16-17]. Distributed generation location based on voltage stability index was proposed in [18]. DG planning studies under market scenario was proposed in [19]. An approach for for DG allocation based on MINLP and voltage stability index was proposed in [20-21]. An analytical approach for DG siting and sizing was proposed in [22]. In this paper, DFIG capability has been determined for real and reactive power output. The capability curves of DFIG has been modelled in an optimization model and impact of wind speed variation for 24 hrs have been considered to obtain the impact on DFIG output. A mixed integer programming based approach for minimizing transmission loss has been proposed to obtain the size, number and location of wind power source. The study has been carried out for IEEE 24 bus test system.

2. DFIG capability limit

A single phase equivalent circuit of DFIG has been considered for obtaining the capability limits of real and reactive power. Figure 1 shows the single-phase equivalent circuit of the DFIG, where U_S is the stator voltage, U_R is the rotor voltage, I_S is the stator current, I_R is the rotor current, R_S is the stator resistance, R_R is the rotor resistance, X_S is the stator reactance, X_R is the rotor reactance, X_M is the mutual reactance, and s is the slip.

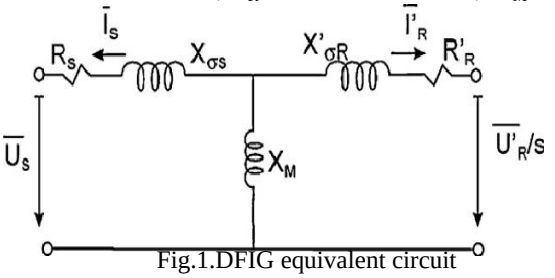

Fig.1.DFIG equivalent circuit

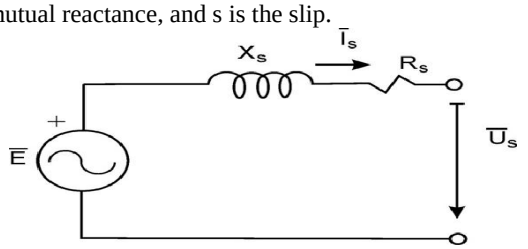

Fig. 2. Stator equivalent circuit

The stator and rotor equations derived from this equivalent circuit are

$$\bar{U}_s = -I_s R_s - jI_s X_s - jI_r X_m \quad (1)$$

$$\bar{U}_r = -I_r R_r - jsI_r X_r - jsI_s X_m \quad (2)$$

$s=\omega_r/\omega_s$, being slip the ratio between rotor to stator pulsation:

By defining the generator internal emf as

$$\bar{E} = -jI_r X_m \quad (3)$$

Substituting (3) into the stator equation in (1):

$$\bar{U}_s = -I_s R_s - jI_s X_s + \bar{E} \quad (4)$$

From equation (4) we can obtain the equivalent circuit of DFIG identical to the synchronous generator classical equivalent circuit as shown in Fig.2.

Stator active and reactive power can be obtained as follows:

$$P_s + jQ_s = 3\bar{U}_s I_s^* \quad (5)$$

From the equivalent circuit, neglecting stator resistance:

$$I_s = (\bar{E} - \bar{U}_s)/jX_s \quad (6)$$

Introducing (5) into (6) and separating into real and imaginary parts:

$$P_s = 3\left(\frac{1}{X_s}\right) E\bar{U}_s \sin\delta \quad (7)$$

$$Q_s = 3\left(\frac{1}{X_s}\right) E\bar{U}_s \cos\delta - 3\left(\frac{\bar{U}_s^2}{X_s}\right) \quad (8)$$

Where, U_S and E are the rms value of the stator voltage and internal emf vectors, respectively, and I is the angle between both vectors.

Rotor active and reactive power can be obtained as follows:

$$P_r + jQ_r = 3\bar{U}_r I_r^* \quad (9)$$

$$P_r + jQ_r = 3[-R_r I_r^2 - jsX_r I_r^2 + js(1/Xs)E_r^*(\bar{E} - \bar{U}s)] \quad (10)$$

Introducing (9) into (10) and separating into real and imaginary parts:

$$P_r = -3s\left(\frac{1}{X_s}\right) E\bar{U}_s \sin\delta \quad (11)$$

$$Q_r = -3s[X_r I_r^2 + \left(\frac{1}{X_s}\right) E\bar{U}_s \cos\delta - \left(\frac{E^2}{X_s}\right)] \quad (12)$$

From equation (7) and (11):

$$P_r = -sP_s \quad (13)$$

The total active power of the DFIG fed into the grid is the sum of stator and rotor active power.

$$P_T = P_s + P_R \quad (14)$$

$$P_R = -sP_S \quad (15)$$

$$P_T = (1 - s)P_S \quad (16)$$

Where, P_T is the total active power of the DFIG fed into the grid, P_S is the stator active power, and P_R is the rotor active power. In opposition to active power, total reactive power fed into the grid is not the addition of stator and rotor reactive power because rotor reactive power cannot flow through the frequency converter. The grid side inverter of the frequency converter has its own reactive power capability, so total reactive power fed into the grid is the sum of the stator and the grid side inverter reactive power.

$$Q_T = Q_S \quad (17)$$

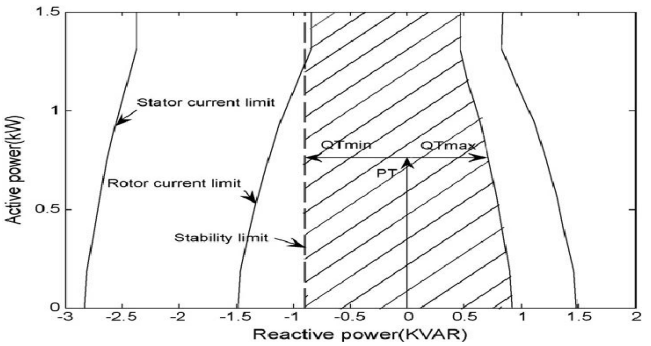

Fig. 3. 1500 kW DFIG capability limits curve

The stator active and reactive power can be expressed as a function of stator and rotor maximum allowable current [41].

$$P_s^2 + Q_s^2 = (3U_s I_s)^2 \quad (18)$$

$$P_s^2 + (Q_s + \frac{3U_s^2}{X_s})^2 = (\frac{3X_m}{X_s} U_s I_r)^2 \quad (19)$$

In the PQ plane (18) represents a circumference centred at the origin with radius equal to the stator rated apparent power. Equation (19) represents a circumference centred at $[-3U_S^2/X_S, 0]$ and radius equal to $3U_S I_R X_M/X_S$. Introducing (16) and (17) into (18) and (19), the stator active and reactive power can be represented as:

$$(\frac{P_T}{1-s})^2 + Q_T^2 = (3U_s I_s)^2 \quad (20)$$

$$(\frac{P_T}{1-s})^2 + (Q_T + \frac{3U_s^2}{X_s})^2 = (\frac{3X_m}{X_s} U_s I_r)^2 \quad (21)$$

According to (20) and (21), the DFIG capability limits can be obtained by considering the stator and rotor maximum allowable currents I_{Smax} and I_{Rmax}. Fig. 3 shows the capability curves of 1500 kW DFIG with its limits, which is obtained by taking into account the maximum stator and rotor currents and the steady state stability limit of the DFIG [49]. In this figure, the solid and dashed curves represent the maximum reactive power that DFIG can generate or absorb corresponding to the stator and rotor maximum allowable currents for terminal voltage U_S = 1.00 pu, respectively. The vertical dotted line at $[-3U_S^2/X_S, 0]$ coordinate represents the stability limit of the DFIG. When the active power that a DFIG should generate is given, the maximum reactive power operation range can be obtained.

3. General OPF formulation in the presence of DFIG

A general objective mixed integer non-linear programming approach considering the total transmission loss for 24 hour has been formulated to find optimal location and number of distributed generators.

$$\text{Min } F\left(x,u,\xi^{\text{int}}\right) \tag{22}$$

Subject to equality and inequality constraints defined as

$$h\left(x,u,\xi^{\text{int}}\right)=0 \tag{23}$$

$$g\left(x,u,\xi^{\text{int}}\right)\le 0 \tag{24}$$

where,

x is state vector of variables V, δ;

u are the control parameters, P_{gi},Q_{gi}, P_{DGi}, Q_{DGi};

ξ^{int} is an integer variable with values {0,1}. The zero value represents absence and one value represents presence of distributed generator in the network.

Objective function F is

$$\text{Min } F\left(x,u,\xi^{\text{int}}\right)=\boldsymbol{P_{ijl}(k)}+\boldsymbol{P_{jil}(k)} \tag{25}$$

The objective function is the total fuel cost of conventional generators only..

The line flows from bus-i to bus-j and bus-j to bus-i are given as:

The line flows from bus-i to bus-j and bus-j to bus-i are given as:

$$P_{ijl}(k)=V_{i,k}^2G_{ij}-V_{i,k}V_{j,k}\left(G_{ij}\cos\left(\delta_{i,k}-\delta_{j,k}\right)+B_{ij}\sin\left(\delta_{i,k}-\delta_{j,k}\right)\right) \tag{26}$$

$$P_{jil}(k)=V_{j,k}^2G_{ij}-V_{i,k}V_{j,k}\left(G_{ij}\cos\left(\delta_{i,k}-\delta_{j,k}\right)-B_{ij}\sin\left(\delta_{i,k}-\delta_{j,k}\right)\right) \tag{27}$$

A. Equality Constraints: Power flow equations corresponding to both real and reactive power balance equations are equality constraints that can be modified in the presence of distributed generation for all the buses as:

$$P_{i,k}=P_{gi,k}+\xi_{i,k}^{\text{int}}*P_{DGi,k}-P_{di,k}\;\forall\, i=1,2,\ldots N_b,k=1,2,...24 \tag{28}$$

$$Q_{i,k}=Q_{gi,k}+\xi_{i.k}^{\text{int}}*Q_{DGi,k}-Q_{di,k}\,\forall\, i=1,2,\ldots N_b,k=1,2,...24 \tag{29}$$

$$P_{i,k}=\sum_{j=1}^{N_b}V_{i,k}V_{j,k}\left[G_{ij}\cos\left(\delta_{i,k}-\delta_{j,k}\right)+B_{ij}\sin\left(\delta_{i,k}-\delta_{j,k}\right)\right]\quad\forall\, i=1,2,\ldots N_b,k=1,2,...24 \tag{30}$$

$$Q_{i,k}=\sum_{j=1}^{N_b}V_{i,k}V_{j,k}\left[G_{ij}\sin\left(\delta_{i,k}-\delta_{j,k}\right)-B_{ij}\cos\left(\delta_{i,k}-\delta_{j,k}\right)\right]\quad\forall\, i=1,2,\ldots N_b,k=1,2,...24 \tag{31}$$

B. Inequality constraints:

(a) *Real power generation limit*: This includes the upper and lower real power generation limit of generators at bus-i

$$P_{gi,k}^{\min}\le P_{gi,k}\le P_{gi,k}^{\max},i=1,2,\ldots N_g,k=1,2,...24 \tag{32}$$

(b) *Reactive power generation limit*: This includes the upper and lower reactive power generation limit of generators and other reactive sources at bus-*i*

$$Q_{gi,k}^{\min} \le Q_{gi,k} \le Q_{gi,k}^{\max}, i = 1,2,\ldots N_q, k = 1,2,....24 \quad (33)$$

(c) *Voltage limit*: This includes the upper and lower voltage magnitude limit $V_i^{\min}, V_i^{\max}$ at bus-*i*

$$V_{i,k}^{\min} \le V_{i,k} \le V_{i,k}^{\max}, i = 1,2,\ldots N_b, k = 1,2,...24 \quad (34)$$

(d) *Phase angle limit*: This includes the upper and lower angle limit $\delta_i^{\min}, \delta_i^{\max}$ at bus-*i*

$$\delta_{i,k}^{\min} \le \delta_{i,k} \le \delta_{i,k}^{\max}, i = 1,2,\ldots N_b, k = 1,2,...24 \quad (35)$$

(e) *Line flow limits*: These constraints represent maximum power flow in a transmission line and are based on thermal and stability considerations. The line flow limit can be written as:

$$\left|S_{ij,k}\right| \le S_{ij,k}^{\max} \quad (36)$$

(f) Two inequality constraints have to be added in an OPF model with distributed generation.

Power generation limit: This includes the upper and lower real power generation limit of generators at bus-*i*

a) Real power generation limit

$$P_{DGi,k}^{\min} \le P_{DGi,k} \le P_{DGi,k}^{\max}, i = 1,2,\ldots N_{DG}, k = 1,2,...24 \quad (37)$$

where, $P_{DGi,k}^{\min}, P_{DGi,k}^{\max}$ are the minimum and maximum generation limit.

b) Reactive power generation limit: This includes the upper and lower reactive power generation limit of distributed generators at bus-*i*

$$Q_{DGi,k}^{\min} \le Q_{DGi,k} \le Q_{DGi,k}^{\max}, i = 1,2,\ldots N_{DG}, k = 1,2,...24 \quad (38)$$

where, $Q_{DGi,k}^{\min}, Q_{DGi,k}^{\max}$ are the minimum and maximum generation limit.

c) Optimal number of distributed generators: This includes the limit on number of maximum distributed generators in the network.

$$N_{DG} = \sum_{i=1}^{N_{DG}} \xi_{i,k}^{\text{int}} \le N_{DG}^{\max} \quad (39)$$

4. Results and discussions

A small wind farm comprising DFIG wind turbines of 1500 kW, with a power installed of 1.5 MW is connected through a rated 23/0.69 kV transformer. The analysis is carried out on IEEE 24-bus system considering different loading condition. Voltage limits are assumed to be within the range 0.95–1.05 p.u. The wind speed curves are obtained and are shown in Fig. 4 for consecutive 24 h of a day. The actual active power outputs of each DFIG in each period are shown in Fig.5 calculated using means of the power curve of each DFIG.

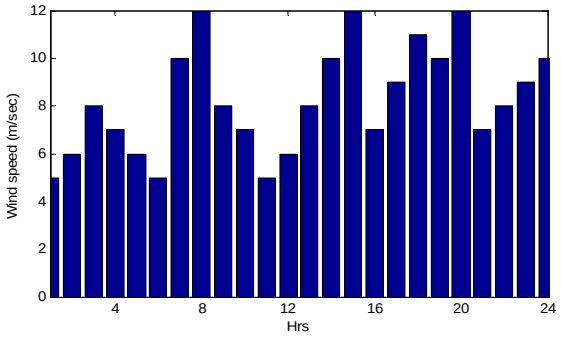

Fig. 4 Curve of wind speed

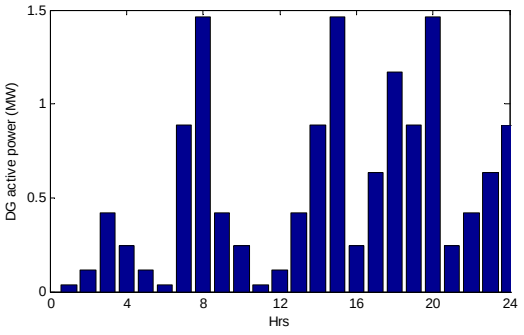

Fig. 5 Actual active power output of wind turbine

DFIG wind turbine output is taken in 24 hour period with the variation in wind speed in each hour of the day. In each hour the average wind speed is used to calculate the output power of DFIG. In period 8, 15 and 20 the DG's output of DFIG is 1.46p.u.MW at the speed of 12 m/sec which is near to the rated capacity. The output power of Wind turbine DFIG is utilised to reduce the transmission loss of IEEE-24 bus system and the effect of wind variation is also find on the location of DG. The system load is 28.5p.u.MW and 5.8p.u.MVar respectively throughout the period of analysis.

The analysis has been carried out considering the following cases:

Case 0: without DG

Case 1: with one DG

Case 2: with two DG

Case 3: with three DG

In case 0 without DG in each period the total real power loss are 0.287712p.u.MW and the total reactive power loss are -2.997p.u.MVar. The results for case 1 (with DG=1) for each hour are given in the following Table 1.

Case 1: with one DG

The Table 1 shows the results obtained for active power loss (PLT), reactive power loss (QLT), total DG size (p.u.MW), total DG size (p.u.MVar) and optimal location of DG.

Table 1: Results of loss, DG size and location with DG for case 1

Hrs	PLT(p.u.MW)	QLT(p.u.MVar)	DG size (p.u.MW)	DG size (p.u.MVar)	DG location
1	0.285764	-3.01487	0.0342	0.01654	4
2	0.281387	-3.0551	0.1161	0.05621	4
3	0.268588	-3.18755	0.4191	0.20298	4
4	0.275334	-3.11423	0.2443	0.11834	4
5	0.281387	-3.0551	0.1161	0.05621	4
6	0.285764	-3.01487	0.0342	0.01654	4
7	0.253519	-3.39118	0.8891	0.43061	3
8	0.242357	-3.56194	1.4649	0.70951	3
9	0.268588	-3.18755	0.4191	0.20298	4
10	0.275334	-3.11423	0.2443	0.11834	4
11	0.285764	-3.01487	0.0342	0.01654	4
12	0.281387	-3.0551	0.1161	0.05621	4
13	0.268588	-3.18755	0.4191	0.20298	4
14	0.253519	-3.39118	0.8891	0.43061	3
15	0.242357	-3.56194	1.4649	0.70951	3
16	0.275334	-3.11423	0.2443	0.11834	4
17	0.261033	-3.29581	0.6363	0.3082	3
18	0.247104	-3.48211	1.1685	0.56594	3
19	0.253519	-3.39118	0.8891	0.43061	3
20	0.242357	-3.56194	1.4649	0.70951	3
21	0.275334	-3.11423	0.2443	0.11834	4
22	0.268588	-3.18755	0.4191	0.20298	4
23	0.261033	-3.29581	0.6363	0.3082	3
24	0.253519	-3.39118	0.8891	0.43061	3

In Table 1, the real and reactive power loss variation and the change in the optimal location in each hour of the day is given. It is observed that when the DG generation is less than 0.5 p.u.MW the location for the optimal result is Bus-4. And when the DG generation is greater than 0.5p.u.MW, the location for the optimal result is at Bus-3. The maximum reduction in active power loss is obtained when the generation is near to the rated power output of the DFIG. In period 8, 15 and 20 the generation is near to the rated power output of DFIG at the speed of 12 m/sec the active power losses are minimum. The Generation schedule for conventional generator and distributed generator are shown in Fig 6(a) and (b). DG active power and reactive power output is shown in Figs. 7(a) and (b). It is observed from Figure 6(a) that at buses 1, 2, 7, 13, 15, 16 and 18 are scheduled at their maximum generation limit. At bus 7, in 1^{st} hour the active generation is 2.8p.u.MW and reduced to its minimum value (i.e. 0.278p.u.MW) in 8^{th} hour. At bus 21, in 1^{st} hour the active generation is 3.038p.u.MW and reduced to 2.348p.u.MW in 8^{th} hour. At bus 22, in 1^{st} hour the active generation is 0.253p.u.MW and reduced to 0.24p.u.MW in 8^{th} hour. At bus 23, in 1^{st} hour the active generation is 4.936.u.MW and reduced to 4.459p.u.MW in 8^{th} hour From 1 to 8 hours the reduction occurs

continuously in active generation of the generator at bus 7, 21, 22 and 23 as the output of DG increases with wind speed. In Fig 6 (b) the reactive power generation of conventional generator is shown. It is observed that the reactive power output of generators at bus 2, 21 and 22 is negative and the rest generators are scheduled at positive reactive power output. It means these generators are absorbing reactive power, whereas the rest generators are supplying reactive power. At bus 1, the reactive generation is 0.1084p.u.MVar in 1st hour which reduced to -0.1604p.u.MVar with increment output in 8th hour.

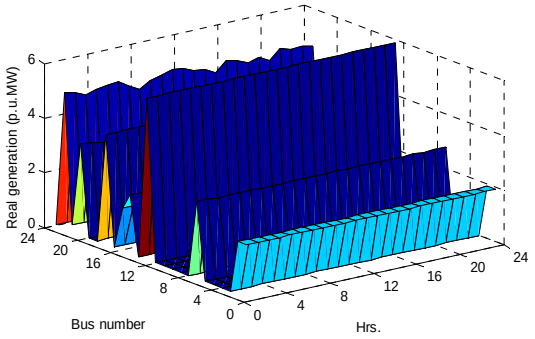

Fig.6 (a) Real power generation (p.u.MW)

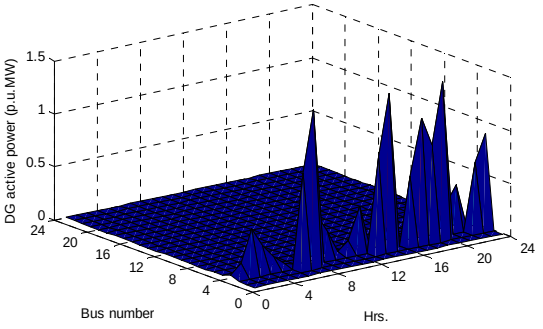

Fig.7 (a) DG active power (p.u.MW)

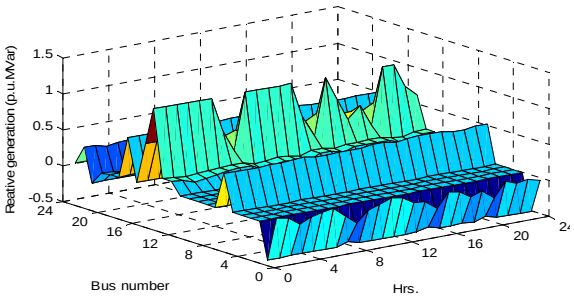

Fig.6 (b) Reactive power generation (p.u.MVar)

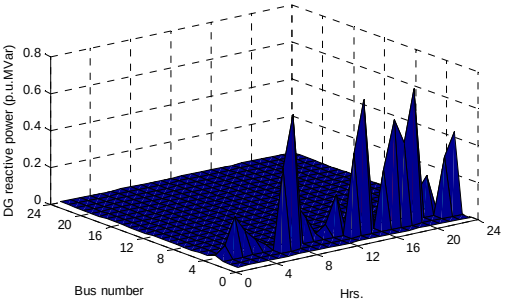

Fig.7 (b) DG reactive power output (p.u.MVar) at 0.9 power factor

At bus 2, the conventional generator is scheduled at its minimum reactive generation (i.e. -0.5p.u.MVar). At bus 7, the reactive generation is 0.509p.u.MVar in 1st hour which reduced to 0.532p.u.MVar with increment in output in 8th hour. At bus 13, the reactive generation is 0.165p.u.MVar in 1st hour which reduced to 0.179p.u.MVar with increment in output in 8th hour. At bus 15, the reactive generation is 1.1p.u.MVar in 1st hour which reduced to 0.139p.u.MVar with increment in output in 8th hour. At bus 18, the reactive generation is 0.588p.u.MVar in 1st hour which reduced to 0.570p.u.MVar with increment in output in 8th hour. At bus 24, the reactive generation is 0.262p.u.MVar in 1st hour which reduced to 0.213p.u.MVar with increment in output in 8th hour. It is clear from this discussion that reactive power of conventional generator is reduced considerably with the increment in DG output.

Case 2: with two DG

The Table 2 total active power loss (PLT), reactive power loss (QLT), total DG size (p.u.MW), total DG size (p.u.MVar) and optimal location of DG.

Table 2 Results of loss, DG size and location with DG=2

Hrs	PLT(p.u.MW)	QLT(p.u.MVar)	DG Size (p.u.MW)	DG size (p.u.MVar)	DG location
1	0.284031	-3.03312	0.0684	0.03308	3,4
2	0.275699	-3.11525	0.2322	0.11242	3,4
3	0.250523	-3.38118	0.8382	0.40596	3,4
4	0.26399	-3.23482	0.4886	0.23668	3,4
5	0.275699	-3.11525	0.2322	0.11242	3,4

6	0.284031	-3.03312	0.0684	0.03308	3,4
7	0.22766	-3.67359	1.7782	0.86122	3,4
8	0.220517	-3.81304	2.9298	1.41902	3,4
9	0.250523	-3.38118	0.8382	0.40596	3,4
10	0.26399	-3.23482	0.4886	0.23668	3,4
11	0.284031	-3.03312	0.0684	0.03308	3,4
12	0.275699	-3.11525	0.2322	0.11242	3,4
13	0.250523	-3.38118	0.8382	0.40596	3,4
14	0.22766	-3.67359	1.7782	0.86122	3,4
15	0.220517	-3.81304	2.9298	1.41902	3,4
16	0.26399	-3.23482	0.4886	0.23668	3,4
17	0.237627	-3.5374	1.2726	0.6164	3,4
18	0.221714	-3.75686	2.337	1.13188	3,4
19	0.22766	-3.67359	1.7782	0.86122	3,4
20	0.220517	-3.81304	2.9298	1.41902	3,4
21	0.26399	-3.23482	0.4886	0.23668	3,4
22	0.250523	-3.38118	0.8382	0.40596	3,4
23	0.237627	-3.5374	1.2726	0.6164	3,4
24	0.22766	-3.67359	1.7782	0.86122	3,4

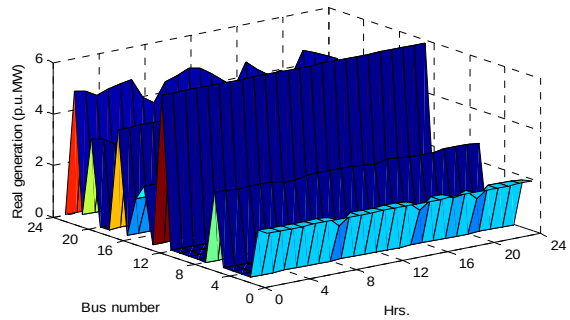

Fig.8 (a) Real power generation (p.u.MW)

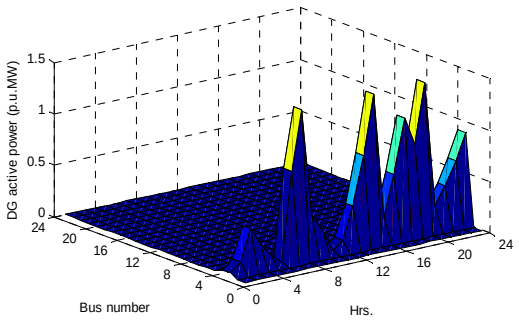

Fig. 9 (a) DG active power (MW)

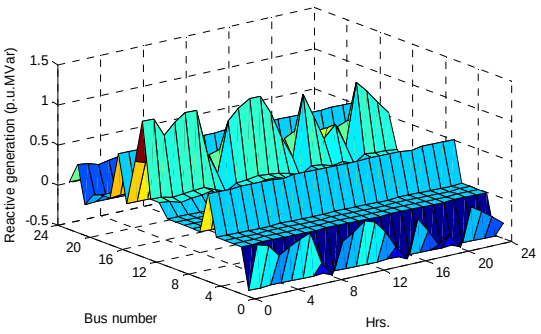

Fig. 8 (b) Reactive power generation (p.u.MVar)

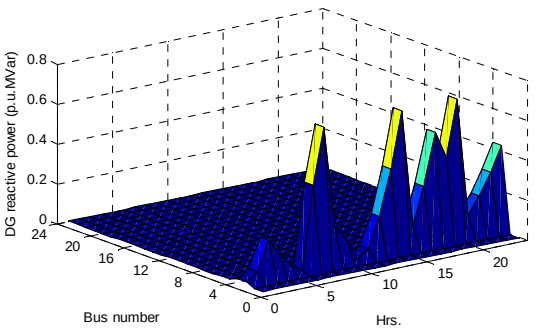

Fig.9 (b) DG reactive power output (MVar) at 0.9 power factor lagging

Table 2 shows the variation in total active and reactive power loss in each hour and the optimal location and size of DG. It is observed that in each hour the optimal location of DG's is at buses 3 and 4. It is observed from Fig 8(a) in case of two DG the real generation of conventional generator is effected at bus 2, 7, 21, 22 and 23, rest generators are scheduled at their maximum generation limit. When, the generation of DG at its rated value there is the maximum reduction in the output of conventional MW generator at buses 2, 7, 21, 22 and 23. This occurs in the periods 8, 15 and 20. The total p.u.MW output of conventional generators is 25.7907. In these periods total active and reactive output of DG is 2.9298p.u.MW and 1.41902p.u.MVar. It is observed that as the DG generation increases the output of conventional generator at bus 23 reduced accordingly. Figure 8(b) shows the p.u.MVar output of conventional generator. It is observed from the figure that at bus 1, the variation in reactive power output

take place with variation DG output in each hour. The reactive power at bus is positive in 1st period when the reactive power of DG is minimum, which become negative as the output of DG reach its rated value.

When the DG reactive power minimum at 0.01654p.u.MVar the reactive power output of conventional generator at bus 1 is 0.091628Mvar and when the reactive power of DG is near to the rated value 0.70951p.u.MVar the conventional p.u.MVar generation at bus 1 is -0.48201p.u.MVar. At bus 15, the considerable variation occurs in reactive power output of the conventional generator. With minimum reactive output of DG the reactive generation at bus 15 is 1.1p.u.MVar and when DG output reaches near to its rated value the reactive generation at this bus become negative that is -0.163p.u.MVar. At bus 2, the reactive generation is constant in each hour and at its minimum generation limit -0.5p.u.MVar. The rest generator buses have the marginal effect on the reactive generation. The optimal location and variation in DG output is shown in Figures 9(a) and 9(b).

Case 3: Results with three DG

The Table 3 shows the results for total active power loss (PLT), reactive power loss (QLT), total DG size (p.u.MW), total DG size (p.u.MVar) and optimal location of DG.

Table 3 Results of loss, DG size and location with DG=3

Hrs	PLT(p.u.MW)	QLT(p.u.Mvar)	DGsize(p.u.MW)	DG size (p.u.MVar)	DG location
1	0.28261	-3.04581	0.1026	0.04962	3,4,5
2	0.271211	-3.15622	0.3483	0.16863	3,4,5
3	0.238719	-3.50153	1.2573	0.60894	3,4,5
4	0.255635	-3.3142	0.7329	0.3550	3,4,5
5	0.271211	-3.15622	0.3483	0.16863	3,4,5
6	0.2826	-3.04581	0.1026	0.04962	3,4,5
7	0.208908	-3.72561	2.6673	1.29183	3,4,10
8	0.213891	-3.65135	4.3947	2.12853	3,4,5
9	0.238719	-3.50153	1.2573	0.60894	3,4,5
10	0.255635	-3.3142	0.7329	0.35502	3,4,5
11	0.28261	-3.04581	0.1026	0.04962	3,4,5
12	0.271211	-3.15622	0.3483	0.16863	3,4,5
13	0.238719	-3.50153	1.2573	0.60894	3,4,5
14	0.208908	-3.72561	2.6673	1.29183	3,4,10
15	0.213891	-3.65135	4.3947	2.12853	3,4,5
16	0.255635	-3.3142	0.7329	0.35502	3,4,5
17	0.222749	-3.61573	1.9089	0.9246	3,4,10
18	0.200454	-3.80842	3.5055	1.69782	3,4,10
19	0.208908	-3.72561	2.6673	1.29183	3,4,10
20	0.213891	-3.65135	4.3947	2.12853	3,4,5
21	0.255635	-3.3142	0.7329	0.35502	3,4,5
22	0.238719	-3.50153	1.2573	0.60894	3,4,5
23	0.222749	-3.61573	1.9089	0.9246	3,4,10
24	0.208908	-3.72561	2.6673	1.29183	3,4,10

In Table 3, total active and reactive power loss in each hour are given. The total active and reactive generation of DG and the location of DG in each hour is also given. The losses are minimum (in 18th hour) when the total p.u.MW DG size is 3.5055p.u.MW and the location of three DG's as given in the table is 3, 4 and 10. When the DG output is at its rated value the total active power loss are 0.213891p.u.MW and the location of DG is 3, 5 and 4. In this hour the losses are slightly higher as compared to the previous one because of the increase in DG power. The conventional MW generation is given in the Figure 10(a) and 10(b). It is observed that at bus 1 the conventional generation is reduced when the DG output is near to its rated value i.e. in hours 8, 15, 20. At bus 2 the reduction in conventional MW generation has been recorded in hours 7,8,14,15,18,19 and 20. Generators at buses 13, 15, 16 and 18 are operated at their maximum generation limit in each hour. The output of generators at buses 7, 21, 22, and 23 varies with the variation in DG output in each hour. In Figure 10(b) the reactive power generations at each bus in each hour is shown. It is observed that the reactive generation at bus 1 is considerably reduced when the output of DG reaches its rated value. At bus 1, in 1st hour the reactive power of conventional generator is positive and its value is 0.091628p.u.MVar which become negative as the output of DG reach its rated value. In hours 8, 15 and 20 the reactive generation at bus 1 is at its minimum limit which is -0.5p.u.Mvar. At bus 7 there is marginal reduction in reactive power output as the output of Dg varies from minimum to its rated value. There is slight increment in reactive power at bus 16 with the variation in DG output from minimum to its rated value. The reactive power

output of the generator at bus 23 reduced with the increment in the DG output. In the 1st hour of analysis, when the DG output is minimum the reactive power of generator at bus 23 is 0.2573p.u.MVar and when the output of DG reach its rated value the reactive generation at bus 23 become -0.2439p.u.Mvar. The reactive power on the remaining buses is affected marginally. The DG active and reactive power is shown in Figure 11(a) and 11(b).

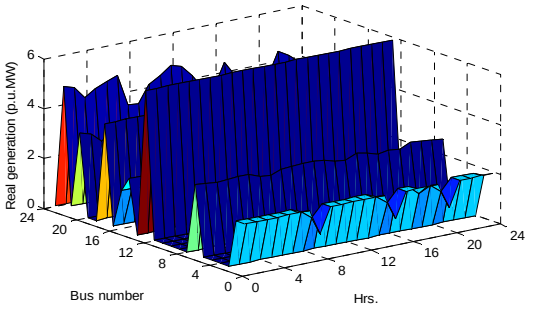

Fig.10 (a) Real power generation (p.u.MW)

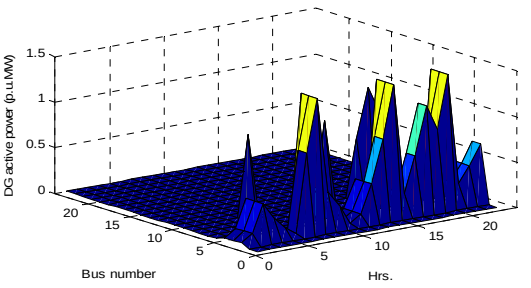

Fig.11 (a) DG active power output (p.u.MW)

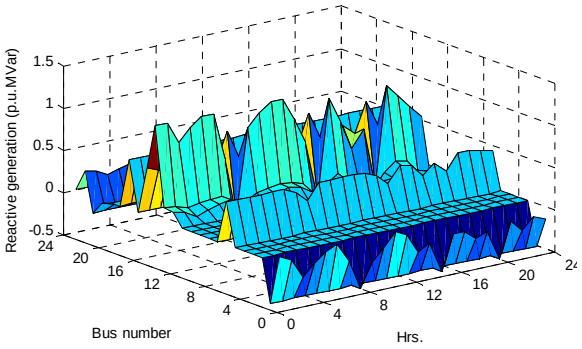

Fig.10 (b) Reactive power generation (p.u.MVar)

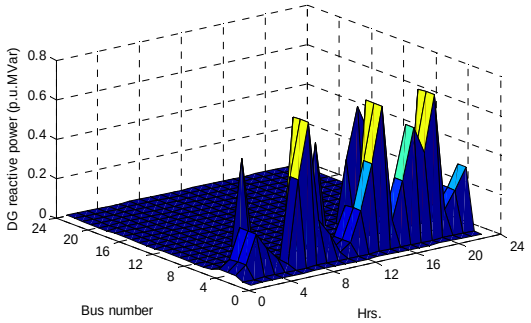

Fig.11 (b) DG reactive power output (p.u.MVar) at 0.9 power factor

The real power loss reduction with wind generator for case1 to 3 is shown in Fig. 12. It is observed that the loss reduces for all cases compared to the case without wind generation integration into the system. For case 3 with three DGs, the loss reduction is more compared to other cases for 24 hours.

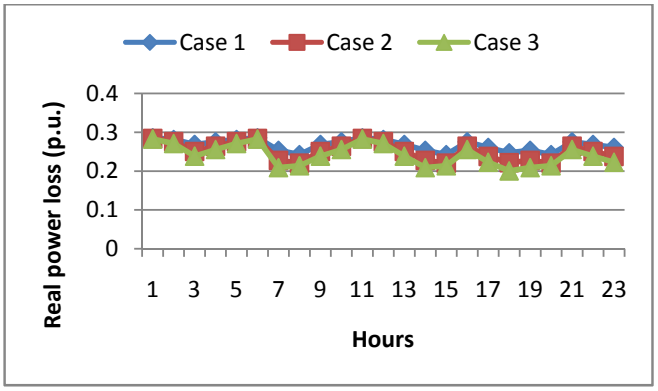

Fig. 12. Real power loss with DGs (p.u.)

4. Conclusions

In this paper, the capability curves of DFIG are obtained and are incorporated in an optimization model. The effect of wind speed variation on the wind power output has been determined and its impact on the transmission loss has been obtained. The optimal DG sizes during each hour and the optimal placement of DGs are obtained. It is observed that as the wind speed increases the output of DFIG also increases and the transmission loss in the system reduces considerably. In this paper, three cases with DG are considered for minimization of transmission loss. It is observed that in case of three DG, the reduction in the transmission loss is higher as compared to the other cases. The voltage profile improves with the presence of DGs for all the cases.

Acknowledgements

The author acknowledges the MHRD New Delhi for providing scholarship during the PhD program in the Department of Electrical Engineering, NIT Kurukshetra.

References

1. "Impact of increasing contribution of dispersed generation on power system-Final Report," CIGRE WG 37-23, Sept. 1998.
2. Ackermann T, Andersson G, and Soder L. Distributed generation: a definition. *Electric Power System Research*, vol. 57, 2001, p. 195-204.
3. El-Khattam W and Salama MMA. Distributed generation technologies, definitions and benefits. *Electric Power System Research*, vol. 71, 2004, p. 119-128.
4. Chiradeja P. and Ramkumar R. An approach to quantify for technical benefits of distributed generation. *IEEE Transactions on Energy Conversion*, vol. 19, no. 4, Dec. 2004, pp. 764-773.
5. Donkelaar M. A survey of solutions and options for integration of distributed generation in electricity supply systems. *Journal of Energy and Environment*, vol. 15, no. 2, 2004, p. 323-332.
6. El-Khattam W, Bhattacharya K, Hegazy Y, and Salama MMA. Optimal investment planning for distributed generation in a competitive electricity markets. *IEEE Trans. on Power Systems*, vol. 19, no. 3, Aug. 2004, p. 1674-1684.
7. Keane E and O'Malley M.. Optimal allocation of distributed generation on distribution networks," *IEEE Trans. on Power Systems*, vol. 20, no. 3, Aug. 2005, p. 1640-1646.
8. Celli G, Ghiani E, Mocci S, and Pilo F. A multi-objective evolutionary algorithm for the sizing and siting for distributed generation," *IEEE Trans. on Power Systems*, vol. 20, no. 2, May 2005, p. 750-757.
9. Borges CLT and Falcao D. M. Optimal distributed generation allocation for reliability, losses, and voltage improvement. *Electric Power and Energy Systems*, vol. 28, 2006, p. 413-420.
10. Acharya N, Mahat P, and Mithulananthan N. An analytical approach for DG allocation in primary distribution network. *Electric Power and Energy Systems*, vol. 28, 2006, pp. 669-678.
11. Harrison GP, Piccolo A, Siano P, and Wallace AR. Hybrid GA and OPF evaluation of network capacity for distribution generation connections. *Electric Power and Energy Systems*, vol. 78, 2008, p. 392-398.
12. Estevej GAJ, Behnke RP, Avila RT, and Vargas LS. A competitive market integration model for distributed generation. *IEEE Transactions on Power Systems*, vol. 22, no. 4, Nov. 2007.
13. Gautam D and Mithulananthan N. Optimal DG placement in deregulated electricity market. *Electric Power System Research*, vol. 77, 2007, p. 1627-1636.
14. Kumar A and Gao Wenzhong. Optimal distributed generation location using mixed integer non-linear programming in hybrid electricity markets. *IET Gener. Transm. Distrib*, pp. 1-18, Vol. 4, No. 2, pp. 281-298, 2010.
15. Ochoa LF, Harrison GP, "Minimizing energy losses: optimal accommodation and smart operation of renewable distributed generation", IEEE Trans Power Syst, vol.26, no.1, 2011, p.198-205.
16. Gomez-Gonzalez M, Lopez A, Jurado F. Optimization of distributed generation system using a new discrete PSO and OPF. Elect Power Syts Res, vol.84, no.1, 2012, pp.174-180.
17. Faruk Ugtanli, Engin Kartepe. Multiple-distributed generation planning under uncertainty and different penetration levels", International Journal of Electrical Power & Energy Systems, vol.46, 22 November 2012, pp.132-144.
18. AmanM.Jasmon J.Mokhlis H.Baka. Optimal placement and sizing of DG based on new power stability index and line losses. Int J Electr Power Energy Syst, vol.43, no-1, 2012, pp.1296-1304.
19. Jain N, Singh SN, Srivastava SC, "A generalized approach for DG planning and viability analysis under market scenario", IEEE Trans Ind Electron, vol.60, no-11, 2013, pp.5075-5085.
20. Kaur, Sandeep Kumbhar V, Jaydev Sharma, "A MINLP technique for optimal placement of multiple DG units in distribution systems", International Journal of Electrical Power & Energy Systems, vol.63, May 2014, pp. 609-617.
21. Masoud Esmaili, Esmail Chaktan Firozjaee, Heidar Ali Shayanfar. Optimal placement of distributed generations considering voltage stability and power losses with observing voltage-related constraints.,International Journal of Applied Energy, vol.113, no.27 September 2013,

p.1252-1260.
22. Viral RK, Khatod DK, .An analytical approach for sizing and siting of DGs in balanced radial distribution networks for loss minimization. International Journal of Electrical Power & Energy Systems, vol.67, May 2015, pp.191-201